Vehicle Lateral Motion Stability Under Wheel Lockup Attacks

Alireza Mohammadi†
University of Michigan-Dearborn
amohmmad@umich.edu

Hafiz Malik
University of Michigan-Dearborn
hafiz@umich.edu

***Abstract*—Motivated by ample evidence in the automotive cybersecurity literature that the car brake ECUs can be maliciously reprogrammed, it has been shown that an adversary who can directly control the frictional brake actuators can induce wheel lockup conditions despite having a limited knowledge of the tire-road interaction characteristics [1]. In this paper, we investigate the destabilizing effect of such wheel lockup attacks on the lateral motion stability of vehicles from a robust stability perspective. Furthermore, we propose a quadratic programming (QP) problem that the adversary can solve for finding the optimal destabilizing longitudinal slip reference values.**

I. Introduction

Electronic Control Units (ECUs) form the backbone of the modern automotive control systems, where protocols such as FlexRay and CAN are utilized to network these embedded devices with each other on one or more buses.

The automotive control systems including their in-vehicle networks (IVNs) and ECUs can be attacked in a variety of ways (see, e.g., [2], [3]). One type of attack geared towards reprogramming the vehicle ECUs and manipulating the car physical behaviors such as steering and braking can be carried out using interfaces such as the vehicle OBD port, Wi-Fi, and cellular networks. For instance, Miller and Valasek [4] carried out such an attack, which was effective on all Fiat-Chrysler vehicles, by reprogramming a V850 chip to disable the car braking system (also, see [5] for other attacks on the brake ECUs). Furthermore, an adversary who can reprogram the firmware of ECUs through the Unified Diagnostic Services (UDS) codified in ISO-14229 [6] can also read live data from the IVN (such as vehicle speed or engine speed). This live data reading capability has been demonstrated in an experimental wireless attack against Tesla vehicles [7]. Therefore, an adversary can affect the stability of motion of a vehicle under attack by means of closed-loop feedback control mechanisms.

Motivated by the possibility of malicious reprogramming of the car braking ECUs, we have investigated the capabilities of an adversary who has taken over these ECUs and would like to induce wheel lockup conditions during braking in our previous work [1]. In particular, we have proposed a feedback attack policy for the frictional brakes that can compensate for the adversary's lack of knowledge of the tire-road interaction dynamics (see Figure 1). The proposed attack policy is capable of regulating the front and/or rear longitudinal tire slips to a small neighborhood of any desired wheel slip value within a small amount of time as determined by the adversary.

Our other work [1], however, did not investigate the effect of such wheel lockup attacks on lateral stability of vehicle motion. Indeed, as evidenced in the vehicle safety literature, wheel lockup can cause severe degradation in vehicle steerability, directional stability, and general control over the car [8] leading to catastrophic road injuries [9]. Therefore, understanding the stability implications of this type of attack policy is of great importance.

In this paper, we formally demonstrate that an adversary who is employing the brake attack policies in our other work [1] can induce instability in vehicle lateral motion. Furthermore, we present a QP that the adversary can solve for finding the "optimal"[1] longitudinal slip reference values for the front and rear wheels capable of destabilizing the vehicle lateral motion. When these reference values are fed into the braking attack policy [1], the instability of the vehicle lateral motion ensues. Our lateral motion robust stability conditions and the ensuing QP rely on the framework by Yi and Tseng [10], which has also been employed for designing aggressive vehicle maneuvers in the work by Yi et al. [11] (also, see the work by Chi and Tsiotras [12]).

Contributions of the paper. This article adds to body of knowledge on cybersecurity in autonomous vehicles in the following ways. First, this work provides a formal analysis of the lateral motion stability of vehicles under wheel lockup attacks in an adversarial setting where the longitudinal slip ratios of either the front, rear, or both wheels can be controlled by an adversary. While the conditions of lateral motion instability have already been derived in the work by Yi and Tseng [10], this paper sheds a new light on these instability results using a graphics-oriented robustness analysis using Mikhailov's plots [13], which have also been employed for robust stability analysis in power systems [14].

[1]Despite the fact that optimality in engineering might imply stable behavior in engineered systems, the adjective "optimal" in this context refers to the adversary's capabilities of inducing unstable dynamical behavior in a vehicle under attack.

Workshop on Automotive and Autonomous Vehicle Security (AutoSec) 2022
24 April 2022, San Diego, CA, USA
ISBN 1-891562-75-4
https://dx.doi.org/10.14722/autosec.2022.23010
www.ndss-symposium.org
†A. Mohammadi is the corresponding author.

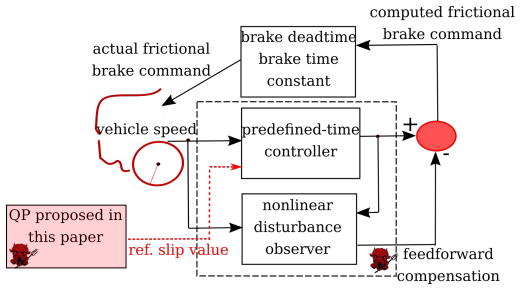

Fig. 1: Block diagram of the attack policy [1].

Furthermore, this paper encodes the vehicle lateral motion instability conditions using a QP. Given the advent of efficient QP-solvers in embedded applications (see, e.g., [15]), such QP formulation has serious safety implications for real-time destabilization of lateral motion of an attacked vehicle.

The rest of this short paper is organized as follows. In Section II, we present some preliminaries about the coupling in-between the vehicle lateral and longitudinal dynamics using the framework developed by Yi and Tseng [10]. Thereafter, we present the conditions under which the lateral dynamics become unstable and shed a new light on these results in terms of tools for robust stability analysis. Next, in Section III, we formulate the obtained lateral motion instability conditions in terms of a QP. Section IV concludes the paper with future research directions.

II. Preliminaries

A. An overview of wheel lockup feedback attack policy

In this section, we present a summary of the results in [1]. For the sake of brevity, the mathematical expressions of the closed-loop feedback attack policy are not presented. Rather, we only review the capabilities of an adversary who is using these attack policies (see [1] for further details).

In the proposed wheel lockup attack policy in [1], it is assumed that the attacker can read from the in-vehicle network and can issue commands to the brake actuators. Under such an assumption, which is well-grounded in the vehicle cybersecurity literature, the attack policy in [1] is capable of issuing closed-loop feedback control-based commands to the vehicle brake actuators such that the trajectories of the vehicle longitudinal dynamics during braking converge to any sufficiently close neighborhood of a desired value for the wheel slips within a finite time interval. Although the attack policy in [1] is focused on inducing lockup on the wheel under attack (corresponding to the desired wheel slip value $\lambda^{\text{ref}} = 1$), the slip values can be regulated to any desired value λ^{ref} with a slight modification of the results in [1].

As it can be seen from Figure 1, the closed-loop feedback attack policy for the frictional brakes in [1] relies on employing a predefined-time controller and a nonlinear disturbance observer (NDOB) [16]. The role of the pre-defined time controller is to drive the trajectories of the vehicle longitudinal dynamics during braking to any sufficiently close neighborhood of a desired value for the wheel slips within a finite time interval when the adversary has a complete knowledge of the tire-road interaction dynamics. When such knowledge is lacking, the role of the NDOB is to compensate for this lack of knowledge via a feedforward compensating command.

B. The coupled longitudinal-lateral motion dynamics

In this section, we briefly present the linearized dynamics that capture the coupling in-between the longitudinal and lateral tire/road friction forces. The interested reader is referred to the work by Yi and Tseng [10] for the complete nonlinear model. Similar to this work, we consider a bicycle model for vehicle dynamics. Figure 2 depicts the schematic of the bicycle model and the parameters pertinent to our stability analysis. To analyze the lateral motion stability of the vehicle, the state variable $\mathbf{x} := [\tan\beta,\ \dot{\psi}]^\top$ is considered (see Figure 2), where $\tan\beta := v_{Gy}/v_{Gx}$. In our derivations, we assume a zero steering angle $\delta_f = 0$ for the sake of brevity. Our analysis can be easily extended to the cases where $\delta_f \neq 0$ (see [10] for further details).

Yi and Tseng in [10] have shown that the linearized dynamics capturing the lateral motion stability about the equilibrium $\mathbf{x} = [0,\ 0]^\top$ are given by

$$\dot{\mathbf{x}} = \mathbf{A}(\lambda_f, \lambda_r)\mathbf{x}, \tag{1}$$

where $\lambda_f \in [0,1]$ and $\lambda_r \in [0,1]$ are the front and rear wheel longitudinal wheel slips. It is known from the vehicle dynamics literature (see, e.g., [8]) that the wheel slip values during braking vary in-between zero and one, where zero and one correspond to free rolling and lockup conditions, respectively. Furthermore, the trace and determinant of the state transition matrix in (1) are given by (see [10] for further details)

$$\begin{aligned}\text{tr}(\mathbf{A}(\lambda_f,\lambda_r)) = \frac{-g}{Lv}\big[b_f g_{fy}(1-b_f\lambda_f)L_2 + b_r g_{ry}(1-b_r\lambda_r)\\ L_1\big] - \frac{gL_1L_2}{I_z Lv}\big[b_f g_{fy}(1-b_f\lambda_f)L_1 + b_r g_{ry}(1-b_r\lambda_r)L_2\big],\end{aligned} \tag{2}$$

and

$$\begin{aligned}\det(\mathbf{A}(\lambda_f,\lambda_r)) = \frac{m}{I_z}\Big(\frac{gL_1L_2}{Lv}\Big)^2\Big\{Lb_f g_{fy}(1-b_f\lambda_f)\big[Lb_r g_{ry}\\ (1-b_r\lambda_r) - \frac{v}{g} + \frac{Lv}{g}b_r g_{ry}(1-b_r\lambda_r)\big]\Big\},\end{aligned} \tag{3}$$

where $L := L_1 + L_2$, and the lengths L_1 and L_2 are shown in Figure 2. Moreover, I_z, m, v, and g denote the moment of inertia, mass, the forward speed of the vehicle, and gravitational acceleration, respectively. Also, $b_i g_{iy}$, $i = r, f$, is given by $b_i g_{iy} F_{iz} = \frac{1}{2}C_{i\alpha}$; and, $C_{i\alpha}$, $i = r,\ f$, denotes the tire corner stiffness coefficient, which can be computed using the approach by Yi et al [10], [17]. Finally, under a static normal load distribution, F_{fz}=$\frac{L_2}{L}mg$ and F_{rz}=$\frac{L_1}{L}mg$.

Remark 2.1: As demonstrated Yi and Tseng [10], if the dynamics given by (1) are asymptotically stable, then the lateral motion will be stable. Given that the wheel lockup attacks in our other work [1] can regulate either λ_f, or λ_r, or both to any desired value, we will find conditions

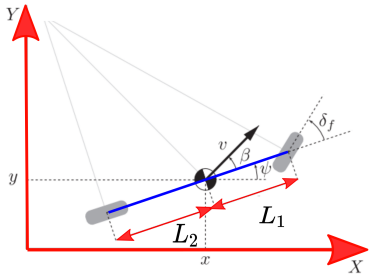

Fig. 2: Bicycle model schematic.

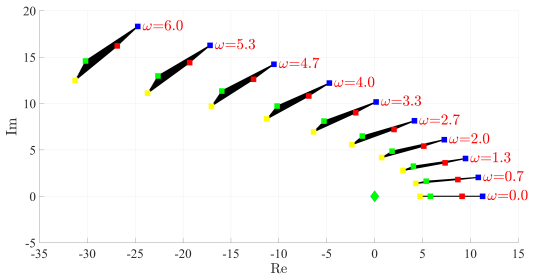

Fig. 3: Mikhailov's plot for $(\lambda_f, \lambda_r) \in [0, 0.03] \times [0, 0.03]$.

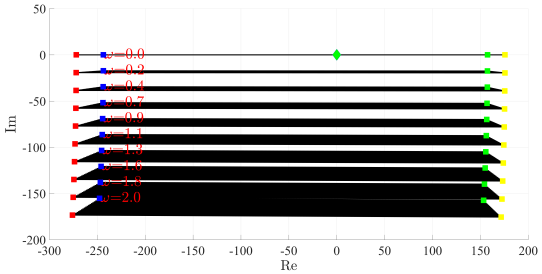

Fig. 4: Mikhailov's plot for $(\lambda_f, \lambda_r) \in [0.95, 1] \times [0.03, 0.05]$.

that guarantee instability of the vehicle lateral motion when $\lambda_f = \lambda_f^{\text{ref}}$, or $\lambda_r = \lambda_r^{\text{ref}}$, or both in Section III.

III. Design/Computation of Destabilizing Longitudinal Wheel Slip Values

In this section, we consider the dynamics in (1) and provide conditions on longitudinal wheel slips λ_f and λ_r such that the lateral motion of the vehicle becomes unstable. Using tools from robust stability literature (see, e.g., [13]), our analysis sheds a new light on these instability results. Later, we will encode these conditions in terms of a QP whose solutions provide the destabilizing slip values (see Figure 1).

A. Robust stability analysis of the lateral motion dynamics

The characteristic polynomial associated with the dynamics in (1) is given by

$$\Delta_{\mathbf{A}(\lambda_f,\lambda_r)}(s) = s^2 - \text{tr}(\mathbf{A}(\lambda_f, \lambda_r))s + \det(\mathbf{A}(\lambda_f, \lambda_r)) \quad (4)$$

where the trace and determinant of $\mathbf{A}(\lambda_f, \lambda_r)$ are given by (2) and (3). The dynamics in (1) are unstable if and only if

$$\text{tr}(\mathbf{A}(\lambda_f, \lambda_r)) \geq 0 \text{ or } \det(\mathbf{A}(\lambda_f, \lambda_r)) \leq 0, \quad (5)$$

Therefore, if the wheel slip values $\lambda_f \in [0, 1]$ and $\lambda_r \in [0, 1]$ satisfy (5), then lateral motion instability in the vehicle ensues.

In general, since λ_f and λ_r are free to vary in the interval $[0, 1]$, the dynamics in (1) can be considered as an uncertain linear time-invariant (LTI) dynamical system, where the characteristic polynomial in (4) belongs to the family

$$\mathcal{F} := \left\{\Delta(s, \mathbf{q}) = s^2 + q_1 s + q_2 : q_1 \in [q_1^-, q_1^+],\ q_2 \in [q_2^-, q_2^+]\right\}, \quad (6)$$

where the uncertain vector $\mathbf{q} = [q_1,\ q_2]^\top$ is given by

$$\mathbf{q}(\lambda_f, \lambda_r) = [-\text{tr}(\mathbf{A}(\lambda_f, \lambda_r)),\ \det(\mathbf{A}(\lambda_f, \lambda_r))]^\top. \quad (7)$$

Therefore, the uncertain parameter vector $\mathbf{q}$ belongs to a subset $\mathcal{D}$ of the operating domain

$$\mathcal{Q} := [q_1^-, q_1^+] \times [q_2^-, q_2^+], \quad (8)$$

where $q_1^- = \min(-\text{tr}(\mathbf{A}(\lambda_f, \lambda_r)))$, $q_1^+ = \max(-\text{tr}(\mathbf{A}(\lambda_f, \lambda_r)))$, $q_2^- = \min(\det(\mathbf{A}(\lambda_f, \lambda_r)))$, and $q_2^+ = \max(\det(\mathbf{A}(\lambda_f, \lambda_r)))$.

According to the so-called "Boundary Crossing Theorem" from robust stability analysis literature (see, e.g., [13]), if the family of polynomials in (6) are stable within a subset $\mathcal{D}$ of the operating domain $\mathcal{Q}$, then as the uncertain parameter vector $\mathbf{q}$ is changing within $\mathcal{D}$, the roots of the lateral dynamics characteristic polynomial $\Delta(s, \mathbf{q})$ cannot jump from the left half to the right half of the complex plane without crossing the imaginary $j\omega$-axis. To formally verify this condition, a graphics-oriented method based on drawing the image set $\Delta(j\omega, \mathcal{D}) = \{\Delta(j\omega, \mathbf{q}) : \mathbf{q} \in \mathcal{D}\}$ can be invoked (see, e.g., [13]). This image set is called the **Mikhailov's plot** associated with the family of uncertain system characteristic polynomials. In particular, we have the following proposition regarding the robust stability of the vehicle dynamics in (1).

Proposition 3.1: Consider the uncertain dynamics in (1) as well as a closed and connected set $\mathcal{D} \subset \mathcal{Q}$. Then, the characteristic polynomials $\Delta(s, \mathbf{q})$ in (6), $\mathbf{q} \in \mathcal{D}$, are robustly stable if and only if (i) there exists a stable $\Delta(s, \mathbf{q})$ in $\Delta(s, \mathcal{D})$; and (ii) for all $\omega \geq 0$, the set $\Delta(j\omega, \mathcal{D}) = \{(j\omega)^2 + q_1(j\omega) + q_2 : \mathbf{q} \in \mathcal{D}\}$ does not contain the origin of the complex plane.

Remark 3.2: According to Proposition 3.1, in order to verify the robust stability of the lateral motion dynamics on a collection of front and rear wheel longitudinal slip values, we need to draw the frequency plot $\Delta(j\omega, \mathcal{D})$ associated with the vehicle lateral motion on a grid of ω in the complex plane. If this frequency plot, which is called the Mikhailov's plot, contains the origin, then there exist front and rear wheel longitudinal slip values that cause instability.

We now apply Proposition 3.1 to the numerical example provided by Yi and Tseng [10], where we have omitted the numerical values for the sake of brevity. Our robust stability analysis approach enables us to predict stability/instability of the lateral motion dynamics without having to compute the trace and determinant of the transition matrix at each pair value of λ_f and λ_r. We consider two cases. In the first case, the front and rear wheel longitudinal slip values both vary in the interval $[0, 0.03]$. It can be easily verified that the characteristic polynomial is asymptotically stable for λ_f=λ_r=0. Figure 3

depicts the Mikhailov's plots in this scenario. Since the origin is encircled by the plots and not contained in $\Delta(j\omega, \mathcal{D})$ for all $\omega \geq 0$, then the lateral motion is robustly stable for $(\lambda_f, \lambda_r) \in [0, 0.03] \times [0, 0.03]$. In the second case, we consider the situation where $(\lambda_f, \lambda_r) \in [0.95, 1] \times [0.03, 0.05]$ corresponding to a locked up front wheel. Figure 4 depicts the Mikhailov's plots in this situation. Since the origin is contained in $\Delta(j\omega, \mathcal{D})$, then we immediately conclude that the dynamics in (1) become unstable for some pair (λ_f, λ_r).

B. QP for computing destabilizing longitudinal slip values

In this section we present a QP whose solutions can be used by an adversary using the wheel lockup attacks in our other work [1]. In particular, the longitudinal slip values resulting from the proposed QP result in instability in the coupled lateral-longitudinal dynamics in (1). To proceed, let us define the vectors

$$\mathbf{\Lambda} := [1 - b_f\lambda_f, 1 - b_r\lambda_r]^\top, \boldsymbol{\zeta}_1 := [b_f g_{fy}, b_r g_{ry}]^\top, \quad (9)$$

Moreover, we define the diagonal matrices Ξ_1:=diag$\{L_2, L_1\}$ and Ξ_2:=diag$\{L_1, L_2\}$, and

$$\mathbf{\Xi} := \mathbf{\Xi}_1 + \frac{L_1 L2}{I_z}\mathbf{\Xi}_2. \quad (10)$$

Subsequently, defining the vector $\boldsymbol{\gamma}^\top := -\boldsymbol{\zeta}_1^\top \mathbf{\Xi}$ and using (2), it is possible to show that the trace of $\mathbf{A}(\lambda_f, \lambda_r)$ can be expressed as $\text{tr}(\mathbf{A}(\lambda_f, \lambda_r)) = -\boldsymbol{\gamma}^\top \mathbf{\Lambda}$. Therefore, from instability conditions in (5), it immediately follows that if $\boldsymbol{\gamma}^\top \mathbf{\Lambda} < 0$, then the lateral motion instability ensues.

In addition to ensuring $\boldsymbol{\gamma}^\top \mathbf{\Lambda} < 0$, the adversary can meet the inequality constraint $\boldsymbol{\gamma}^\top \mathbf{\Lambda} < 0$, while minimizing $\det(\mathbf{A}(\lambda_f, \lambda_r))$. This observation is formally stated in the following proposition, where a QP for finding destabilizing slip values is provided.

Proposition 3.3: Consider the QP associated with the coupled longitudinal-lateral dynamics in (1)

$$\begin{aligned} \min_{\mathbf{\Lambda}} \quad & \mathbf{\Lambda}^\top \begin{bmatrix} 0 & \frac{1}{2} \\ \frac{1}{2} & 0 \end{bmatrix} \mathbf{\Lambda} - \frac{v}{gLb_f b_r g_{ry} g_{fy}} \boldsymbol{\zeta}_1^\top \mathbf{D} \mathbf{\Lambda} \\ \text{s.t.} \quad & \boldsymbol{\gamma}^\top \mathbf{\Lambda} < 0, \\ & \mathbf{\Lambda}_{\text{lb}} \leq \mathbf{\Lambda} \leq \mathbf{\Lambda}_{\text{ub}}, \end{aligned} \quad (11)$$

where $\mathbf{D} = \text{diag}\{1, -1\}$, $\mathbf{\Lambda}_{\text{lb}} = [1 - b_f, 1 - b_r]^\top$, and $\mathbf{\Lambda}_{\text{ub}} = [1, 1]^\top$. Consider the solution $\mathbf{\Lambda}^*$ to the QP in (11). Then, the longitudinal slip value vector $[\lambda_f, \lambda_r]^\top = [1, 1]^\top - \text{diag}\{\frac{1}{b_f}, \frac{1}{b_r}\}\mathbf{\Lambda}^*$ results in unstable dynamics in (1).

The proof is straightforward and omitted for the sake of brevity. The obtained destabilizing reference values from the QP in (11) can then be utilized by the adversary for executing the wheel lockup attack proposed in [1].

Remark 3.4: In case that one of the slip values cannot be directly controlled by the adversary, an equality constraint should be added to the QP. For instance, if the rear wheel longitudinal slip is equal to λ_{r0} and cannot be controlled, then the equality constraint $[0, \frac{-1}{b_r}]^\top \mathbf{\Lambda} = \frac{-1}{b_r} + \lambda_{r0}$ should be included in the QP given by (11).

Remark 3.5: The appeal of the QP formulation in (11) for an adversary, who is interested in causing the most possible damage to a vehicle under attack, is rooted in the emergence of customized ECUs that can efficiently solve numerical optimization problems in real-time (see, e.g., [15]).

IV. Concluding Remarks and Future Research Directions

Motivated by the recent development of braking attack policies, this paper investigated the analysis and design of longitudinal wheel slip values that result in instability of vehicle lateral motion. Future research directions will include developing QP-based solutions for finding destabilizing wheel slip values under uncertainty, utilizing these results in the context of driving simulators such as CARLA [18], and investigating the implications for cyberattacks against platoons of connected vehicles [19].

ACKNOWLEDGMENT

This work is supported by NSF Award 2035770.

References

[1] A. Mohammadi, H. Malik, and M. Abbaszadeh, "Generation of CAN-based wheel lockup attacks on the dynamics of vehicle traction," in *Workshop on Automotive and Autonomous Vehicle Security (AutoSec) 2022*, 2022, doi: https://dx.doi.org/10.14722/autosec.2022.23025.

[2] K. Kim, J. S. Kim, S. Jeong, J.-H. Park, and H. K. Kim, "Cybersecurity for autonomous vehicles: Review of attacks and defense," *Comput. Secur.*, p. 102150, 2021.

[3] K. Koscher, A. Czeskis, F. Roesner, S. Patel, T. Kohno, S. Checkoway, D. McCoy, B. Kantor, D. Anderson, H. Shacham *et al.*, "Experimental security analysis of a modern automobile," in *The Ethics of Information Technologies*. Routledge, 2020, pp. 119–134.

[4] C. Miller and C. Valasek, "Remote exploitation of an unaltered passenger vehicle," *Black Hat USA*, vol. 2015, no. S 91, 2015.

[5] S. Fröschle and A. Stühring, "Analyzing the capabilities of the CAN attacker," in *Eur. Symp. Res. Comput. Secur.*, 2017, pp. 464–482.

[6] I. O. for Standardization (ISO). (2020) ISO 14229-1:2020 Road vehicles Unified diagnostic services (UDS) Part 1: Application layer. [Online]. Available: https://www.iso.org/standard/72439.html

[7] S. Nie, L. Liu, and Y. Du, "Free-fall: Hacking Tesla from wireless to CAN bus," *Briefing, Black Hat USA*, vol. 25, pp. 1–16, 2017.

[8] T. D. Gillespie, *Fundamentals of vehicle dynamics*. Society of automotive engineers Warrendale, PA, 1992, vol. 400.

[9] M. J. Giummarra, B. Beck, and B. J. Gabbe, "Classification of road traffic injury collision characteristics using text mining analysis: Implications for road injury prevention," *PloS one*, vol. 16, no. 1, p. e0245636, 2021.

[10] J. Yi and E. H. Tseng, "Nonlinear stability analysis of vehicle lateral motion with a hybrid physical/dynamic tire/road friction model," in *ASME Dyn. Syst. Contr. Conf. (DSCD)*, vol. 48920, 2009, pp. 509–516.

[11] J. Yi, J. Li, J. Lu, and Z. Liu, "On the stability and agility of aggressive vehicle maneuvers: a pendulum-turn maneuver example," *IEEE Trans. Contr. Syst. Technol.*, vol. 20, no. 3, pp. 663–676, 2011.

[12] C. You and P. Tsiotras, "High-speed cornering for autonomous off-road rally racing," *IEEE Trans. Contr. Syst. Technol.*, vol. 29, no. 2, pp. 485–501, 2021.

[13] J. Ackermann, *Robust control: the parameter space approach*. Springer Science & Business Media, 2002.

[14] J. Zhou, P. Shi, D. Gan, Y. Xu, H. Xin, C. Jiang, H. Xie, and T. Wu, "Large-scale power system robust stability analysis based on value set approach," *IEEE Trans. Power Syst.*, vol. 32, no. 5, pp. 4012–4023, 2017.

[15] M. M. Brugnolli, B. A. Angélico, and A. A. M. Laganá, "Predictive adaptive cruise control using a customized ECU," *IEEE Access*, vol. 7, pp. 55 305–55 317, 2019.

[16] S. Li, J. Yang, W.-H. Chen, and X. Chen, *Disturbance observer-based control: methods and applications*. CRC press, 2014.

[17] J. Li, Y. Zhang, and J. Yi, "A hybrid physical-dynamic tire/road friction model," *ASME J. Dyn. Syst. Meas. Contr.*, vol. 135, no. 1, p. 011007, 2013.
[18] A. Dosovitskiy, G. Ros, F. Codevilla, A. Lopez, and V. Koltun, "CARLA: An open urban driving simulator," in *Conf. Robot Learning*. PMLR, 2017, pp. 1–16.
[19] R. Merco, F. Ferrante, and P. Pisu, "A hybrid controller for DOS-resilient string-stable vehicle platoons," *IEEE Trans. Intell. Transp. Syst.*, vol. 22, no. 3, pp. 1697–1707, 2021.